**MRS Advances © 2018 Materials Research Society**
**DOI: 10.1557/adv.2018.479**

# Investigation of BMI-$PF_6$ Ionic Liquid/Graphite Interface Using Frequency Modulation Atomic Force Microscopy

Harshal P. Mungse, Takashi Ichii, Toru Utsunomiya, and Hiroyuki Sugimura

*Department of Materials Science and Engineering, Kyoto University, Kyoto 606-8501, Japan*

*ABSTRACT*

*Structural analysis on interfaces between ionic liquids (ILs) and solid substrates is an important study for not only the basic fundamental aspects but also many technological processes. In the present work, we utilized frequency modulation atomic force microscopy (FM-AFM) based on a quartz tuning fork sensor to elucidate the structure of interface between 1-butyl-3-methylimidazolium hexafluorophosphate (BMI-$PF_6$) IL and highly ordered pyrolytic graphite (HOPG) surface. It was observed that this IL form solvation layers at their interface, with ~0.5-0.57 nm thickness of each layer. We have compared our experimental results with previously reported results from molecular dynamics simulation study, and combination of classical molecular dynamics and density functional theory calculations in order to understand the IL/HOPG interface.*

## INTRODUCTION

Room temperature ILs are new class of ionic salts which contains organic cations and organic/inorganic anions. In recent years, they attracted great attention of the various research communities due to their remarkable properties such as high ion conductivity, low vapor pressure, high thermal stability, and high electrochemical stability [1,2]. Due to these properties their demand increased in many technological applications such as catalysis, coating, electrolyte for batteries and solar cells, crystal growth processes, as a solvent in synthetic processes, in the field of water splitting to produce hydrogen, and neat or base lubricants in tribology [3-14]. However, for these applications, a detailed understanding of molecular-scale properties of ILs at the IL/solid interfaces is essential because important processes occur at their interface. The IL exhibit different behavior at the interface as compare to bulk. An organization of IL molecules depends not only on the structure of cations/anions but also on nature of substrate materials, on which they organized [15,16]. Overall the interfacial properties depend on various factors such as charge on the substrate surface, chemical nature, geometry of surface, and chemical

structure of IL molecules. In order to improve efficiency of technological processes, the knowledge about IL/solid interfaces is required.

In recent years, large number of efforts have been carried out to understand the structure of liquid molecules at liquid/solid interfaces by theoretical as well as various experimental approaches such as surface force apparatus, sum frequency generation, scanning tunneling microscopy (STM) and atomic force microscopy (AFM) techniques [17-19]. More recently, FM-AFM has been developed to achieve true atomic-resolution imaging, and in order to understand the nature of liquid molecules at liquid/solid interfaces. Previously, an obtaining atomic-resolution images of the samples in liquid using FM-AFM was difficult, because of low force sensitivity due to the low $Q$ factor of cantilever [20]. Fukuma et al. have overcome this difficulty and obtained molecular resolution images in liquid with a developed multienvironment FM-AFM [21,22]. The use of small oscillation amplitude of the cantilever found to be effective for enhancing the sensitivity to short range interaction forces, which allowed to obtained atomic-resolution imaging in liquid [23,24]. The FM-AFM measurements of calcite in ambient and liquid environments have been reported using a sensor, based on a quartz tuning fork, so-called a qPlus sensor [25]. Most recent advancement in FM-AFM have imaged an atomic-resolution three-dimensional (3D) images of electrolyte solution near the solid surface [26]. It has been used to generate real-space images of individual DNA molecules and 3D hydration structure around them [27]. These studies revealed that, the FM-AFM technique immerged as powerful tool and has a great impact in the various research field like surface science and nanotechnology. Furthermore, this fascinating tool was used to investigate IL/solid interfaces. ILs layering structure were also analysed by force curve measurements using contact mode AFM [28,29]. Generally, in FM-AFM, Si based cantilevers are used as its force sensor. The quality factor ($Q$) of Si cantilever in viscous ILs is heavily suppressed ($\sim$1), which leads to low force sensitivity. Yokota and co-workers successfully imaged the layered structure at IL/mica and IL/graphite interfaces by using the low-noise optical beam deflection system for Si cantilevers [30]. In contrast, Ichii et al. used a qPlus sensor with sharpened metal tip, instead of Si cantilever. High $Q$ factor was maintained by immersing only tip apex in IL, resulting high force sensitivity, and true atomic-resolution of KCl(100) in viscous IL was achieved [31].

Carbon based materials such as activated carbon, graphene, functionalized graphene oxide, graphite, and carbon nanotubes are important components in the energy related applications. These materials have been applied in several advanced applications in environmental science, catalysis, sensors, and nanodevices [32-35]. In addition to this, these materials have been widely used in electrochemical double layer supercapacitors due to their remarkable physical and chemical properties [36-38]. Graphitized surfaces are popular in applications of ILs. Hence, structural analysis on the interfaces between ILs and carbon-based materials would be helpful for future many potential applications. Recently, the electrical double layer of ILs at the single layer, few layer graphene, and graphite have studied by measuring force curves by AFM [29,39]. BMI-$PF_6$ IL/HOPG or graphene interface are widely studied by using molecular dynamics simulation, and combination of classical molecular dynamics and density functional theory calculations [40-42]. However, understanding of this interface from experimental results is still limited.

Herein, we report the investigation of BMI-$PF_6$ IL/HOPG interface by using FM-AFM technique. The BMI-$PF_6$ IL was selected in this study because it has many applications in the catalysis, as a solvent in the synthetic processes, in crystal growth processes, and as electrolyte for supercapacitors [9-13]. The adsorption of BMI-$PF_6$ IL on HOPG surface and presence of solvation layers at their interface are

demonstrated. We also studied the solvation structure of another IL 1-butyl-3-methylimidazolium tris(pentafluoroethyl)trifluorophosphate (BMI-FAP) on BMI-FAP/HOPG interface.

## EXPERIMENTAL DETAILS

In this study, we used FM-AFM instrument based on a commercial AFM (JEOL JSPM-5200). An original AFM head was replaced by home-built AFM head for a qPlus sensor. At first, we prepared qPlus sensor which was used as force sensor, by attaching one prong of the commercially available quartz tuning fork (STATEK Co. TFW-1165) to the substrate with the help of epoxy adhesive. The tip was made from tungsten wire by electrochemical etching method and then glued to other prong of tuning fork [31]. The photograph of prepared qPlus sensor is shown in figure 1(a). The resonance frequency and spring constant of the tuning fork before tip attachment were 32.768 kHz and 1884 $Nm^{-1}$ respectively. However, after attaching the tungsten tip, resonance frequency was decreased to 14 kHz. The detail about our FM-AFM instrument with block diagram is discussed in the reference [43].

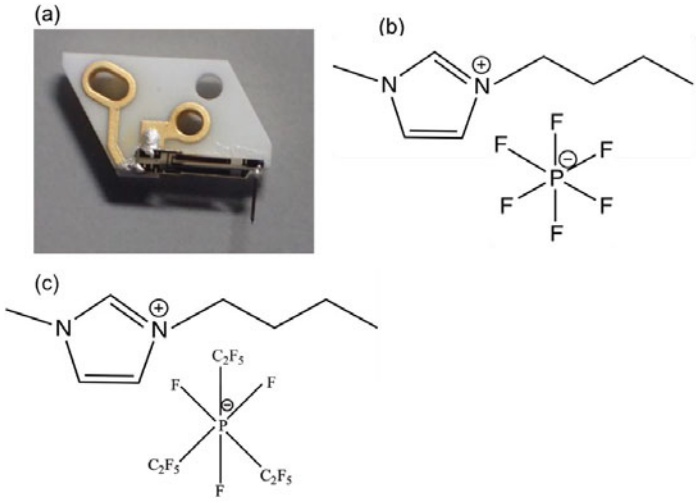


**Figure 1.** (a) photograph of qPlus sensor, (b & c) molecular structures of BMI-$PF_6$, & BMI-FAP ILs, respectively.

BMI-$PF_6$ IL [Tokyo Chemical Industry Co., LTD, > 98 %] and BMI-FAP (Merck) were purchased and used without further purification. The molecular structures of ILs are shown in figure 1(b&c). HOPG substrate (SPI-2 grade) (10 x10 x 2 mm) was purchased from SPI supplies. In sample preparation, HOPG substrate was cleaved inside the drying chamber by using scotch tape and then immediately the IL droplet (0.2 µL) was placed on the HOPG surface by using syringe. This

sample was used for interfacial study using FM-AFM. All the data including topographic image were obtained at room temperature.

## RESULTS AND DISCUSSION

We measured *Q* factor of qPlus sensor in air and viscous BMI-$PF_6$ IL (308 cP), which were found to be 750 and 41, respectively. In this study, during experiment, only the sharp tip apex was inserted into the IL so that *Q* factor was kept high and high force sensitivity was achieved. When the tip apex was sufficiently closed to the sample surface, the resonance frequency of the qPlus sensor generally changed due to tip-to-sample interaction. The frequency shift (Δf) of the force sensor was responsible to generate actual topographic image of the sample in FM-AFM.

In order to confirm the presence of solvation layers of IL on the BMI-$PF_6$/HOPG interface experimentally, a Δf vs tip-to-sample distance curve was obtained. Figure 2(a) shows the oscillatory profile with three peaks and characteristic spacing between the peaks were found to be 0.5-0.57 nm. We were performed Δf vs tip-to-sample distance measurements several times, and observed consistence results. In our previous report on IL/solid interface, Δf vs tip-to-sample distance curves showed oscillatory profiles with two or three peaks, which revealed the presence of solvation layers [43]. Thus, in this study, each oscillation in the figure 2(a) correspond to IL layer. Hu Jun et al. studied the structure of BMI-$PF_6$ IL on graphite surface by molecular dynamic simulation [40]. They reported that calculated average thickness value of IL layer was 0.6 nm. From our experimental study, the obtained values of IL layer thickness (spacing between the peaks) well matches with calculated values from the simulation studies. The dimensions of BMI cations (L=1.1, W=0.55, H=0.28 nm) and anions (diameter = 0.51nm) were reported in the previous study [44]. By taking these dimensions and IL layer thickness in consideration, we assume that the cations lie flat or parallel to the HOPG surface because the obtained values of IL layer thickness are comparable only when the cation lies flat (H=0.28 nm, diameter of anion = 0.51nm) to the HOPG surface. Because of π- π interaction between the imidazolium ring and HOPG surface, the possibility of presence of cations layer near the HOPG surface is higher [40].

Moreover, we have chosen another IL (BMI-FAP), in which anion is different than those in BMI-$PF_6$. The molecular structure of BMI-FAP IL is shown in figure 1(c). We obtained Δf vs tip-to-sample distance curve on BMI-FAP/HOPG interface as shown in figure 2(b). In this, only one peak was observed which correspond to the IL layer near the HOPG surface. Interestingly, the thickness of this layer (~0.58 nm) is comparable with the obtained thickness value of BMI-$PF_6$ IL layers. Recently, Yokota et al. reported the structural properties of 1-butyl-3-methylimidazolium bis(trifluoromethanesulfonyl)imide (BMI-TFSI) on mica and graphite interfaces by molecular dynamics simulation [45]. In this, they also suggested that, imidazolium ring and molecular axis of cation are parallel to the graphite surface at the first layer. In another approach, from molecular dynamics simulation study, the mass and electron density profile of IL showed that the first peak adjacent to graphene or graphite surface is considerably higher as compare to others corresponding to solid-like IL bottom layer [40]. In our study, by considering the IL layer thickness values and higher frequency shift near the surface, we assume that the possibility of presence of cations layer near the HOPG surface is higher.

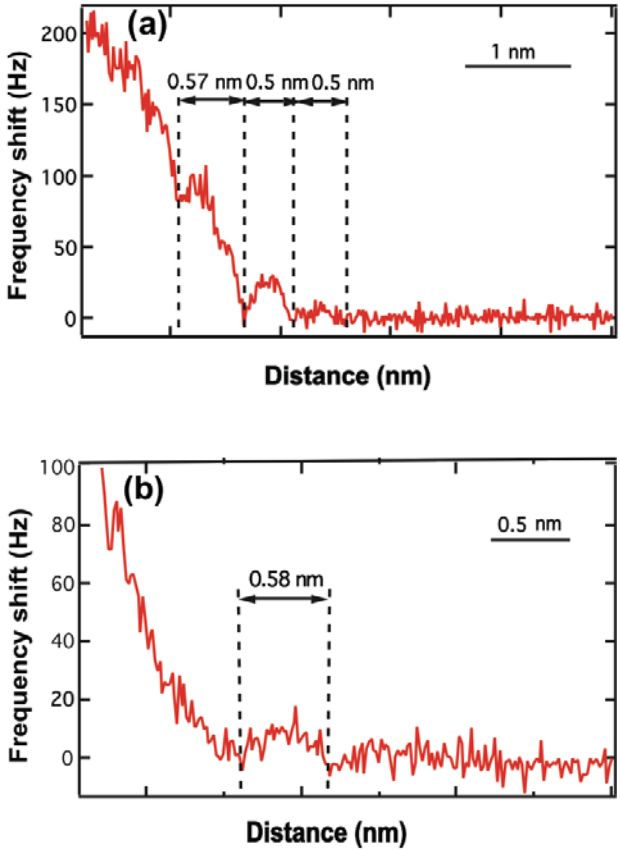


**Figure 2.** Frequency shift vs tip-to-sample distance curve obtained on (a) BMI-$PF_6$/HOPG [A = 1.9 nm], and (b) BMI-FAP/HOPG [A = 0.2 nm] interfaces, respectively.

Furthermore, we have carried out the topographic imaging of HOPG surface in BMI-$PF_6$ IL. The bright protrusions were observed on the HOPG surface as shown in figure 3(a). If the bright spots are originated due to the adsorption of cations then thickness should be 0.28 nm. However, the measured height of bright spot was found to be 0.53 nm, which is shown in the cross-sectional plot (figure 3b) along the line displayed in image (a). This result indicate that the observed bright spots are not because of lying cation on the HOPG surface. The thickness value (0.53 nm) coincides with the values obtained from Δf curves (in this study) and IL layer thickness reported in the simulation studies [40,42]. It is noted that these bright

protrusions were observed only when the imaging was carried out in IL. Moreover, in order to confirm the bright spots are originated due to adsorption of ILs, we have been carried out imaging many times and observed similar thickness values which are found in the range of IL layer thickness. Thus, bright spots on HOPG surface were originated because of adsorbed IL. Yokota et al. studied the BMI-$BF_4$/HOPG and BMI-TFSI/HOPG interface by FM-AFM imaging using Si cantilevers [30]. They have shown the layered structure of IL molecules on HOPG substrate and observed that the thickness of layered structure is in good agreement with the ion-pair size of ILs. In our study, the thickness value (0.53) was found to be smaller compared to theoretical ion-pair diameter (0.7 nm). It is known that the properties and molecular structure of the liquid molecules at the interface are different compared to bulk [46]. The theoretical ion-pair diameter of the IL was just calculated by assuming bulk IL and density with cubic packing geometry and was not based on a precise computational simulation method. This may be one of the reason due to which the IL layer thickness value was found to be smaller than the theoretical ion-pair diameter. However, this thickness value also agrees well with the IL layer thickness values obtained by simulation study. Thus, our results support the results obtained by simulation studies. In the FM-AFM, a qPlus sensor might detect the molecules just adjacent to the surface as compared to the Si cantilevers because of higher stiffness of a qPlus sensor (stiffness for Si = 40 N/m, qPlus sensor =1884 N/m). We observed many materials with atomic-resolution in ILs using qPlus sensor as a force sensor in FM-AFM [31,43]. This suggest that a qPlus sensor have an ability to detect the substrate surface as well as adsorbed molecules near the surface in ILs.

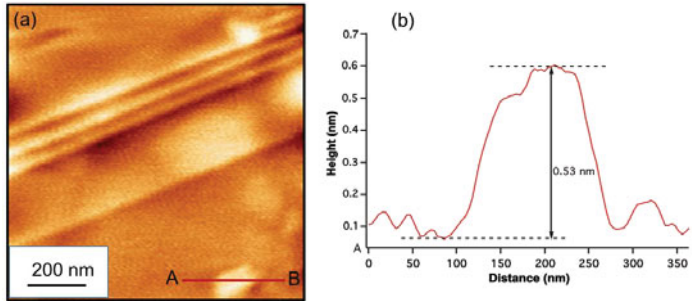


**Figure 3.** (a) FM-AFM topographic image of HOPG surface obtained in BMI-$PF_6$ [$\Delta f = +19$ Hz, $A = 1.3$ nm], (b) cross-sectional plot obtained along the displayed line in image (a).

## CONCLUSIONS

In conclusion, we have analysed the interface between BMI-$PF_6$ IL and HOPG surface by $\Delta f$ vs tip-to-sample distance curve measurement using FM-AFM. The presence of IL solvation layers with thickness of 0.5-0.57 nm of each layer were

confirmed. Our experimental results demonstrating the presence of solvation layers on the interface were found to be consistent with the results obtained by other research groups using molecular dynamics simulation and density functional theory calculations. We also carried out topographic imaging on HOPG surface in IL and physisorbed IL molecules on the HOPG surface were detected.

## ACKNOWLEDGEMENTS

This work was supported by a Grant-in-Aid for Scientific Research B (No. 17H02787) from Japan Society for Promotion of Science (JSPS). Author H.P.M. is grateful to JSPS for postdoctoral research fellowship.

## REFERENCES

1. M. Galinski, A. Lewandowski, I. Stepniak, *Electrochim. Acta* **51**, 5567–5580 (2006).
2. D. R. MacFarlane, N. Tachikawa, M. Forsyth, J. M. Pringle, P. C. Howlett, G. D. Elliott, J. H. Davis, et al. *Energy Environ. Sci.*, **7**, 232-250 (2014).
3. T. Torimoto, T. Tsuda, K. Okazaki, S. Kuwabata, *Adv. Mater.* **22**, 1196-1221 (2010).
4. H. Liu, Y. Liu, J. Li, *Phys. Chem. Chem. Phys.* **12**, 1685–1697 (2010).
5. K. R. J. Lovelock, I. J. Villar-Garcia, F. Maier, H. P. Steinrück, P. Licence, *Chem. Rev.* **110**, 5158–5190 (2010).
6. M. Armand, F. Endres, D. R. MacFarlane, H. Ohno, B. Scrosati, *Nat. Mater.* **8**, 621-629 (2009).
7. H. P. Steinrück, *Phys. Chem. Chem. Phys.* **14**, 5010– 5029 (2012).
8. I. Minami, *Molecules* **14**, 2286-2305 (2009).
9. P. Suarez, V. Selbach, J. Dllius, S. Einloft, Electrochim. Acta, **42**, 2533 (1997).
10. T. Welton, *Chem. Rev.* **99**, 2071-2083 (1999).
11. C. Cadena, J. L. Anthony, J. K. Shah, T. I. Morrow, J. F. Brennecke, E. J. Maginn, *J. Am. Chem. Soc.* ***126*** **(16),** 5300–5308 (2004).
12. W. Lu, A. Fadeev, B. Qi, E. Smela, B. Mattes, J. Ding, G. Spinks, J. Mazurkiewicz, D. Zhou, G. Wallace, D. Macfarlane, S. Forsyth, M. Forsyth, *Science* **297**, 983–987 (2002).
13. S. Kato, Y. Takeyama, S. Maruyama, Y. Matsumoto, *Cryst. Growth Des.* **10**, 3608-3611 (2010).
14. Y. Zhou, J. Qu, *ACS Appl. Mater. Interfaces* **9**, 3209-3232 (2017).
15. R. Atkin, G. G. Warr, *J. Phys. Chem. C* **111**, 5162-5168 (2007).

16. H. Li, F. Endres, R. Atkin, *Phys. Chem. Chem. Phys.* **15**, 14624– 14633 (2013).
17. C. Aliaga, C. S. Santos, S. Baldelli, *Phys. Chem. Chem. Phys.* **9**, 3683-3700 (2007).
18. M. Mezger, H. Shiröder, H. Reichert, S. Schramm, J. S. Okasinski, S. Schöder, V. Honkimäki, M. Deutsch, B. M. Ocko, J. Ralston, et al. *Sicence* **322,** 424–428 (2008).
19. R. Atkin, S. Z. El Abedin, R. Hayes, L. H. S. Gasparotto, N. Borisenko, F. Endres, *J. Phys. Chem. C* **113**, 13266-13272 (2009).
20. P. K. Hansma, J. P. Cleveland, M. Radmacher, D. A. Walters, P. E. Hillner, M. Bezanilla, M. Fritz, D. Vie, H. G. Hansma, *Appl. Phys. Lett.* **64**, 1738-1740 (1994).
21. T. Fukuma, K. Kobayashi, K. Matsushige, H. Yamada, *Appl. Phys. Lett.* **86**, 193108 (2005).
22. T. Fukuma, M. Kimura, K. Kobayashi, K. Matsushige, H. Yamada, *Rev. Sci. Instrum.* **76**, 053704 (2005).
23. T. Fukuma, K. Kobayashi, K. Matsushige, H. Yamada, *Appl. Phys. Lett.* **87**, 034101 (2005).
24. K. Suzuki, N. Oyabu, K. Kobayashi, K. Matsushige, H. Yamada, *Appl. Phys. Exp.* **4**, 125102 (2011).
25. E. Wutscher, F. Giessibl, *Rev. Sci. Instrum.* **82**, 093703 (2011).
26. D. M.-Jimenez, E. Chacon, P. Tarazona, R. Garcia, *Nat. Commun.* **7**, 12164, (2016).
27. K. Kuchuk, U. Sivan, *Nano Lett.* **18**, 2733-2737 (2018).
28. R. Hayes, N. Borisenko, M. K. Tam, P. C. Howlett, F. Endres, R. Atkin, *J. Phys. Chem. C* **115**, 6855-6863 (2011).
29. J. M. Black, D. Walters, A. Labuda, G. Feng, P. C. Hillesheim, S. Dai, P. T. Cummings, S. V. Kalinin, R. Proksch, N. Balke, *Nano Lett.* **13**, 5954-5960 (2013).
30. Y. Yokota, T. Harada, K.-I. Fukui, *Chem. Commun.* **46**, 8627-8629 (2010).
31. T. Ichii, M. Negami, H. Sugimura, *J. Phys. Chem. C* **118**, 26803–26807 (2014).
32. V. Georgakilas, J. N. Tiwari, K. C. Kemp, J. A. Perman, A. B. Bourlinos, K. S. Kim, R. Zboril, *Chem. Rev.* **116**, 5464-5519 (2016).
33. A. C-Valdez, M. S. P. Shaffer, A. R. Boccaccini, J. Phys. Chem. B **117**, 1502-1515 (2013).
34. V. Georgakilas, A. Demeslis, E. Ntararas, A. Kouloumpis, K. Dimos, D. Gournis, M. Kocman, M. Otyepka, R. Zboril, *Adv. Funct. Mater.* **25**, 1481—1487 (2015).
35. S. J. Peng, L. L. Li, X. P. Han, W. P. Sun, M. Srinivasan, S. G. Mhaisalkar, F. Y. Cheng, Q. Y. Yan, J. Chen, S. Ramakrishna, *Angew. Chem. Int. Ed.* **53**, 12594-12599 (2014).

36. E. Frackowiak and F. Beguin, *Carbon* **40**, 1775–1787 (2002).
37. D. N. Futaba, K. Hata, T. Yamada, T. Hiraoka, Y. Hayamizu, Y. Kakudate, O. Tanaike, H. Hatori, M. Yumura and S. Iijima, *Nat. Mater.*, **5**, 987–994 (2006).
38. Y. Zhu, S. Murali, M. D. Stoller, K. J. Ganesh, W. Cai, P. J. Ferreira, A. Pirkle, R. M. Wallace, K. A. Cychosz, M. Thommes, D. Su, E. A. Stach and R. S. Ruoff, *Science* **332**, 1537–1541 (2011).
39. L. A. Jurado, R. M. E-Marzal, *Sci. Rep.* **7**, 1-12 (2017).
40. M. Sha, F. Zhang, G. Wu, H. Fang, C. Wang, S. Chen, Y. Zhang, J. Hu, *J. Chem. Phys.* **128**, 134504 (2008).
41. E. Paek, A. J. Park, G. S. Hwang, *J. Electrochem. Soc.* **160** (1), A1-A10 (2013).
42. S. A. Kislenko, I. S. Samoylov, R. H. Amirov, *Phys. Chem. Chem. Phys.* **11**, 5584-5590 (2009).
43. T. Ichii, M. Fujimura, M. Negami, K. Murase, H. Sugimura, *Jpn. J. Appl. Phys.* **51**, 1-5 (2012).
44. J. M. Black, M. Zhu, P. Zhang, R. R. Unocic, D. Guo, M. B. Okatan, S. Dai, P. T. Cummings, S. V. Kalinin, G. Feng, N. Balke, *Sci. Rep.* **6**, 1-12 (2016).
45. Y. Yokota, H. Miyamoto, A. Imanishi, K. Inagaki, Y. Morikawa, K.-I. Fukui, *Phys. Chem. Chem. Phys.* **20**, 6668-6676 (2018).
46. J. Israelachvili, H. Wennerstrom, *Nature* **379**, 219-225 (1996).